Impact of the Spring North Atlantic Oscillation on the Northern Hemisphere Tropical Cyclone Genesis Frequency

Leying Zhang[1], Xiting Yang[1] and Jiuwei Zhao[2]*[†]

[1]College of Biology and the Environment, Joint Innovation Center for Modern Forestry Studies, Nanjing Forestry University, Nanjing, China, [2]Institute of Climate and Application Research, Nanjing University of Information Science and Technology, Nanjing, China

A majority of studies have documented basin-dependent factors for predicting interannual variability of tropical cyclone genesis frequency (TCGF) over basins. In this study, we find that the spring North Atlantic Oscillation (NAO) has cross-basin impacts on summer and autumn TCGF over the whole North Hemisphere. The positive NAO suppresses the TCGF in the North Atlantic (NA) but promotes the TCGF in the North Pacific (NP) *via* modulating the large-scale environment parameters and vice versa. The positive NAO in spring can induce negative sea surface temperature (SST) anomalies in the NA, which persists into summer *via* the ocean memory. The negative SST anomalies cool the overlying atmosphere and damp the precipitation, leading to a low-level anti-cyclonic circulation and thereby counteracting the TCGF over the NA in summer and autumn. The southerly anomaly west of the anti-cyclonic circulation increases the SST and precipitation over the northeast Pacific in summer. Accordingly, a cyclonic circulation appears western NP *via* Gill response and sustains by the warm advection *via* the air–ocean positive feedback, which devotes the NP TCGF in summer and autumn. The composite results in high-resolutions numerical model from Coupled Model Intercomparison Project Phase 6 further verify the relationship between the spring NAO and TCGF.

Keywords: North Atlantic oscillation, tropical cyclones genesis frequency, north hemisphere, preceding influence, high-resolutions numerical model

INTRODUCTION

Tropical cyclone (TC) often associates with destructive weather, resulting in enormous death and property damage (Kossin et al., 2016; Peduzzi et al., 2012; Schultz and Cecil, 2009). Thus, numerous efforts are directed to monitor and predict the TC genesis frequency (TCGF) variability. The TCGF exhibits a distinct interannual variation (Chan and Xu, 2009), extensively associated with the local sea surface temperature (Li, 2012; Zhao and Wang, 2019). Li (2012) showed that the TCGF in the western North Pacific (NP) tends to increase during the summer of a developing El Niño, while it decreases during the summer of a decaying El Niño. Mei et al. (2019) revealed that a 1°C increase in SST of the main TC development region produces 7.05 ± 1.39 more hurricanes in the North Atlantic (NA) from 100 ensembles of high-resolution atmospheric simulations. Besides the local SST, remote tropical SST forcing can also modulate the interannual variability of TCGF (Cao et al., 2016; Du et al., 2011; Tao et al., 2012; Wang et al., 2014; Yu et al., 2021). Patricola et al. (2016) suggested that Atlantic

tropical cyclones are suppressed during El Niño. Zhan et al. (2011) reported that warm eastern Indian Ocean SST anomaly suppresses the TCGF in the western NP through the large-scale atmospheric circulation and barotropic energy conversion in summer. Yu et al. (2016) found that the negative NA SST in summer can induce a local negative heating anomaly and trigger a low-level anomalous westerly in the tropical Indian Ocean. The westerly anomaly cools the SST and suppresses convection *in situ*, inducing anomalous westerlies over the western NP, and thereby increases the TCGF there.

In addition to the tropical forcing, extratropical forcing plays active roles in the TCGF interannual variability. Choi and Byun (2010) found that more TCs form over east of 150°E and recurve in the east during a strong summer Arctic Oscillation. Wang and Wang (2021) proposed that during a strong South Asian high year, the related upper-level convergence favors descending motion and low-level divergence in the South China Sea, decreasing mid-level humidity and low-level vorticity and thus suppressing TCGF there. Zhou and Cui (2014) showed that during a strong summer North Atlantic Oscillation (NAO), an anomalous cyclonic circulation appears in the western NP and benefits the TCGF there. This relationship features a significant interdecadal shift, which becomes significant after 1980.

The preceding extratropical forcing could also serve as a prediction on the TCGF. Zhang et al. (2020) indicated that East Asian Jet Stream significantly enhances the subsequent TCGF in the NA through a Rossby wave train. A strong North Pacific Oscillation in spring induces a tripole SST pattern over the NP, which subsequently results in an enhanced western NP monsoon trough, thereby fostering the TCGF (Chen et al., 2015a). A strong positive NP Victoria mode in spring benefits a strengthened western NP monsoon trough and weakened western Pacific subtropical high *via* the wind-evaporation-SST feedback, leading to an enhanced (suppressed) TCGF in the eastern (western) western NP (Pu et al., 2019). Choi and Cha (2017) showed that a positive June NAO indicates that more July–August TCs occurs in the northwestern region of western NP, while the positive April–May NAO also devotes to the June–September TC in the western NP (Zhou and Chen, 2020).

Note that no matter the simultaneous or preceding relationship, previous studies mostly focus on the impact of large-scale circulation on the TC in one specific basin. From a single-factor analysis model, Elsner and Kocher (2000) noted that the NAO has a statistically simultaneous link to the global TCGF. That is, the annual NAO is negatively correlated with the TCGF in Atlantic, while it is positive in other oceanic basin. However, how the NAO influences the global TCGF has not been followed up. The NAO is traditionally characterized by the sea-level pressure difference between Iceland and the Azores (Walker, 1924) and is closely related to the strength and direction of westerly winds and storm tracks at mid-high latitude (Nie et al., 2020; Wettstein and Wallace, 2009). The spring NAO could persist its influence through the memory of SST anomalies (Wu et al., 2009) and modulate the global climate and atmospheric circulation in the following seasons (Du et al.,

2019; Ham et al., 2013; Zuo et al., 2012). What is more, the spring NAO could modulate the following ENSO evolution and western Pacific subtropical high intensity, which are both closely related to the TCGF (Chen et al., 2014; Wang et al., 2013; Wang and Wang, 2021). These strongly suggest that NAO may exert significant influences on the global TCs in the following seasons, which is not clear yet.
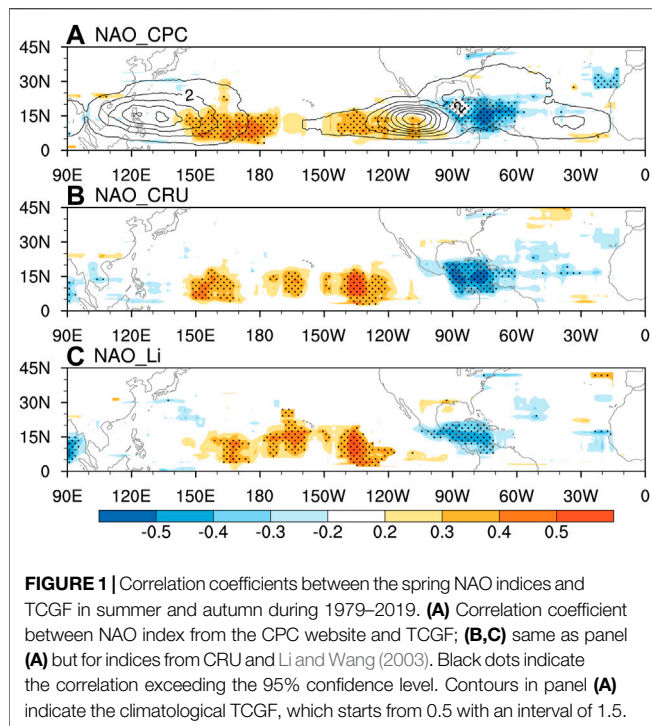
In this study, we aim to ascertain the influence of the spring NAO on the North Hemisphere (NH) TCGF in summer and autumn and explore the associated mechanism. **Section 2** introduces the data and methods. **Section 3** describes the relationship between the spring NAO and North Hemisphere TCGF in the following seasons. The associated mechanism is given in **Section 4**. **Section 5** is a summary and discussion.

DATA AND METHODS

Data
We used the 6-hourly NH TC best-track dataset from the International Best Track Archive for Climate Stewardship version 4 (IBTrACS v4; https://www.ncei.noaa.gov/data/international-best-track-archive-for-climate-stewardship-ibtracs/v04r00/access/netcdf/) to obtain TC information, including TC central position (in longitude and latitude) and intensity in terms of maximum sustained near-surface wind speed of each TC. The TC genesis location is defined as the central position where a TC reaches 35 knots for the first time. Since 85% of the TCs form during June–November each year, we focused on the summer and autumn in this study (Murakami et al., 2015). In addition, TCs over the North Indian Ocean mainly form in the pre-monsoon (April and May) and the post-monsoon (October and November) seasons (Chen et al., 2015b); thus, the TCGF over the North Indian Ocean was not included in this study.

The monthly NAO index was downloaded from the National Oceanic and Atmospheric Administration (NOAA) Climate Prediction Center (CPC) website (https://www.cpc.ncep.noaa.gov/products/precip/CWlink/pna/nao.shtml; Barnston and Livezey, 1987) for the observational data. The indices from Climate Research Unit (CRU) (https://crudata.uea.ac.uk/cru/data/nao/nao.dat; Jones et al., 1997), calculated according to Li and Wang (2003), which is the difference of monthly normalized sea level pressure (SLP) averaged over the longitudes of 80°W–30°E between 35°N and 65°N, are also used to verify the robust relationship between the NAO and TCGF. The spring NAO index is defined as the mean of monthly NAO indices averaged from March to May. The monthly atmospheric reanalysis is from the fifth-generation European Center for Medium-Range Weather Forecasts atmospheric reanalysis of the global climate (ERA5), including sensible heat flux, latent heat flux, SLP, precipitation, winds, vorticity, relative humidity, and air temperature with a $1.0° \times 1.0°$ horizontal resolution (https://cds.climate.copernicus.eu/cdsapp#!/search?type=dataset; Hersbach et al., 2020). The monthly SST is obtained from the Hadley Center Global Sea Ice and SST (HadISST) with a resolution of $1.0° \times 1.0°$ (https://www.metoffice.gov.uk/hadobs/hadisst2/data/download.html; Rayner, 2003). All the data were

FIGURE 1 | Correlation coefficients between the spring NAO indices and TCGF in summer and autumn during 1979–2019. **(A)** Correlation coefficient between NAO index from the CPC website and TCGF; **(B,C)** same as panel **(A)** but for indices from CRU and Li and Wang (2003). Black dots indicate the correlation exceeding the 95% confidence level. Contours in panel **(A)** indicate the climatological TCGF, which starts from 0.5 with an interval of 1.5.

FIGURE 2 | Time series of the spring NAO index from the CPC and area-averaged TCGF in summer and autumn and their correlation coefficient (r). **(A)** The spring NAO index and the TCGF area averaged over the NA (5°N–25°N, 90°W–20°W); **(B)** same as panel **(A)**, but for TCGF over the NP (5°N–25°N, 100°E–90°W).

from 1979 to 2019, and their linear trends were removed in advance.

Provided by Coupled Model Intercomparison Project Phase 6 (CMIP6), here, we also used datasets with high spatio-temporal resolutions from the European Centre for Medium-Range Weather Forecasts (ECMWF). The present-day simulation of ECMWF has a spatial resolution of 0.5° and 6-hourly output interval forced by the observed daily SST data from 1979 to 2014, which also contain five members that are integrated with a slight difference of the initial conditions. The five members are from r2i1p1f1, r3i1p1f1, r4i1p1f1, r5i1p1f1, and r6i1p1f1 runs in the ECMWF. The SLP, winds, and relative humidity were used to define the TCGF and verify its relationship with the NAO in the CMIP6. The NAO index in the CMIP6 was calculated according to Li and Wang (2003). Following previous studies (Murakami and Wang, 2010; Zhao et al., 2020a; Zhao et al., 2020b), the TCs were extracted from the high-resolution ECMWF datasets based on criteria below: first, a low pressure center was traced, but the SLP isobars were not necessary to be closed; second, the surface/850-hPa winds were not <15/17 m s^{-1} at least one time in its lifespan, and the absolute value of vorticity at 850 hPa was larger than 5×10^{-5} s^{-1}; third, the TC lifetime should be longer than 1.5 days; and last but optional, the warm core of a TC should exist in the range of 1,200–2,400 km at 300–500 hPa. We consider the TC genesis as the winds speed larger than 15 m s^{-1} for the first time in the lifespan of a TC.
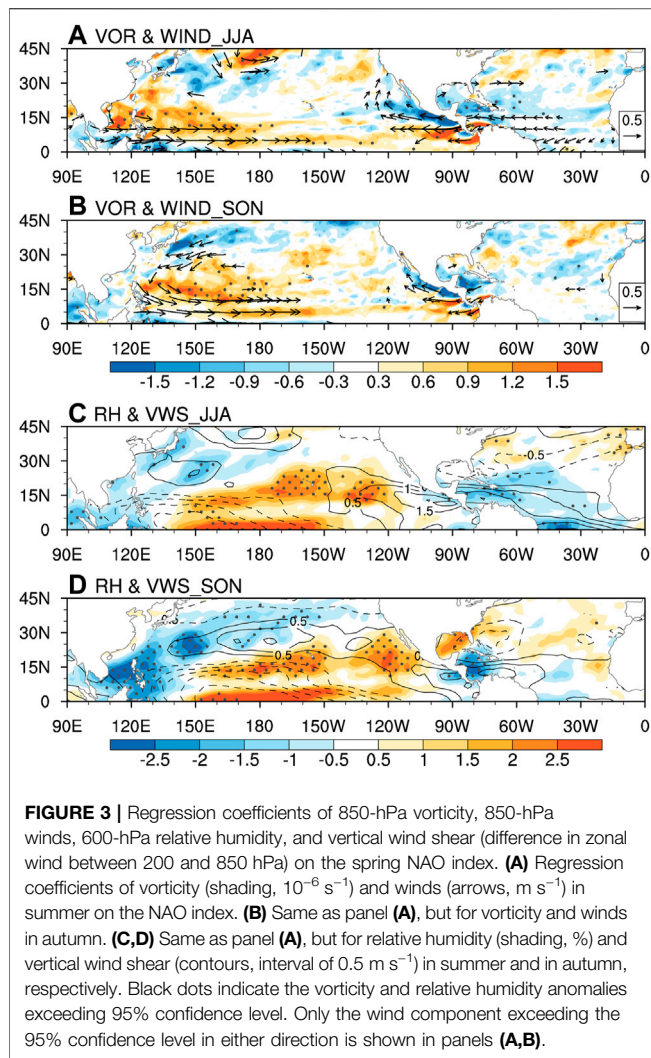
Tropical Cyclone Genesis Frequency Definition

According to the kernel density method of TCGF (Lu and Xiong, 2019), the NH domain is meshed into 1° × 1° grid box, and then,
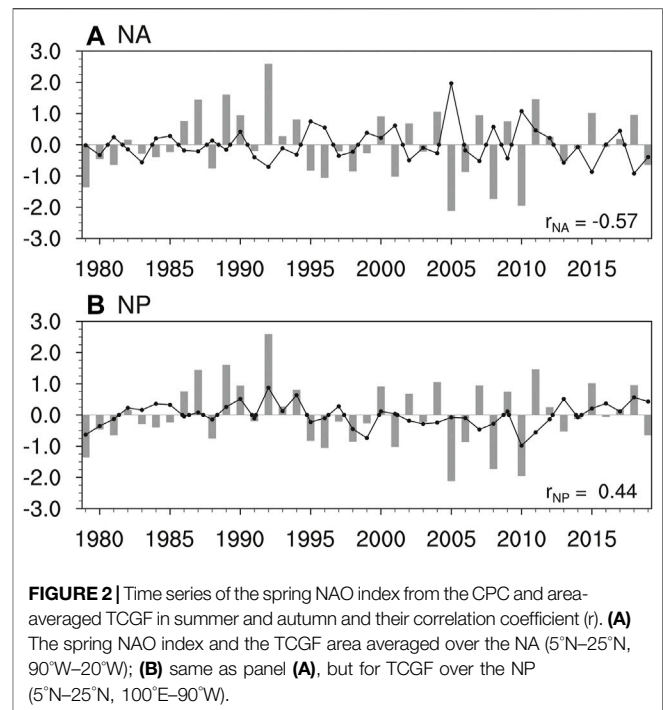
the TCGF in each grid box is counted as the sum of the TCs formed in an area of 10° in the zonal direction and 5° in the meridional direction centered at this grid box. This method, as a smoother, cannot only reduce the possible uncertainty due to the scattering nature of TC genesis or bias of genesis location in the TC data but also establish a stable relationship between the observed TCGF and the related environmental factors. Since the synoptic waves, such as equatorial Rossby waves, mixed-Rossby-gravity wave, and easterly wave, or other types of synoptic disturbances that trigger TC genesis have scales of about 2,000 km in the zonal direction and e-folded in the meridional direction, we chose a 20° × 10° domain in this study (Chen and Huang, 2009).

RELATIONSHIP BETWEEN THE NORTH ATLANTIC OSCILLATION AND TROPICAL CYCLONE GENESIS FREQUENCY

Figure 1 displays the correlation coefficients between the spring NAO indices from three definitions and TCGF from observational data in summer and autumn. The high correlation coefficients for all three NAO indices over the NA and NP show that the summer–autumn TCGFs are closely related to the spring NAO. During a positive NAO, the TCGF over the NA is remarkably reduced, while those over the NP could experience a tremendous increase in the following tropical cyclone (hurricane) seasons. This is consistent with the simultaneous correlation between the annual NAO and TCGF in Elsner and Kocher (2000). The out-of-phase relationship between TCGF over the North Atlantic and the North Pacific is also found in the previous studies (Maue, 2009; Wang and Lee, 2009; Wang et al., 2016). Note that the significant coefficient

FIGURE 3 | Regression coefficients of 850-hPa vorticity, 850-hPa winds, 600-hPa relative humidity, and vertical wind shear (difference in zonal wind between 200 and 850 hPa) on the spring NAO index. **(A)** Regression coefficients of vorticity (shading, 10^{-6} s^{-1}) and winds (arrows, m s^{-1}) in summer on the NAO index. **(B)** Same as panel **(A)**, but for vorticity and winds in autumn. **(C,D)** Same as panel **(A)**, but for relative humidity (shading, %) and vertical wind shear (contours, interval of 0.5 m s^{-1}) in summer and in autumn, respectively. Black dots indicate the vorticity and relative humidity anomalies exceeding 95% confidence level. Only the wind component exceeding the 95% confidence level in either direction is shown in panels **(A,B)**.

FIGURE 4 | Regression coefficients of SST on the spring NAO index. **(A)** Regression coefficients of spring SST (shading, °C) on the NAO index. **(B,C)** Same as panel **(A)**, but for summer and autumn SST, respectively. Black dots indicate the SST anomalies exceeding 95% confidence level. Arrows in panel **(A)** are the regression coefficients of 1,000-hPa winds (arrows, ms^{-1}) on the spring NAO index. Only the wind component exceeding the 95% confidence level in either direction is shown. Regression coefficient of the heat flux (positive downward, contours, interval of 10^{-5} J m^{-2}) over the North Atlantic on the SST index in the key regions (red box) is imposed in panel **(B)**.

concentrates on the Gulf of Mexico and Northeast Pacific (**Figure 1A**). We further calculated the correlation coefficients between the spring NAO index from CPC and TCGF area averaged over the whole tropical NA (90°W–60°W, 5°N–25°N) and NP (100°E–90°W, 5°N–25°N); they were −0.57 and 0.44, respectively, all exceeding the 95% confidence level (**Figure 2**). This confirms the robust relationship between the spring NAO and the TCGF in summer and autumn. Moreover, the 3-month time lag coefficient indicates that the spring NAO could potentially be used to predict the TCGF over the NA and NP.

Large-scale environment parameters are considered to make great contributions in the TCGF (Gray, 1979; Wang and Wang, 2021; Zhang et al., 2020). **Figure 3** shows the regression coefficients of vorticity, winds, relative humidity, and vertical wind shear on the spring NAO. For NA, the negative vorticity and relative humidity anomalies with the positive anomalous vertical wind shear appearing in summer and autumn during a positive NAO are all unfavorable for the TCGF. In contrary, the positive vorticity, the positive relative humidity, and the negative vertical wind shear anomalies favor the occurrence of the TC in the NP. Thus, the spring NAO could modulate the large-scale
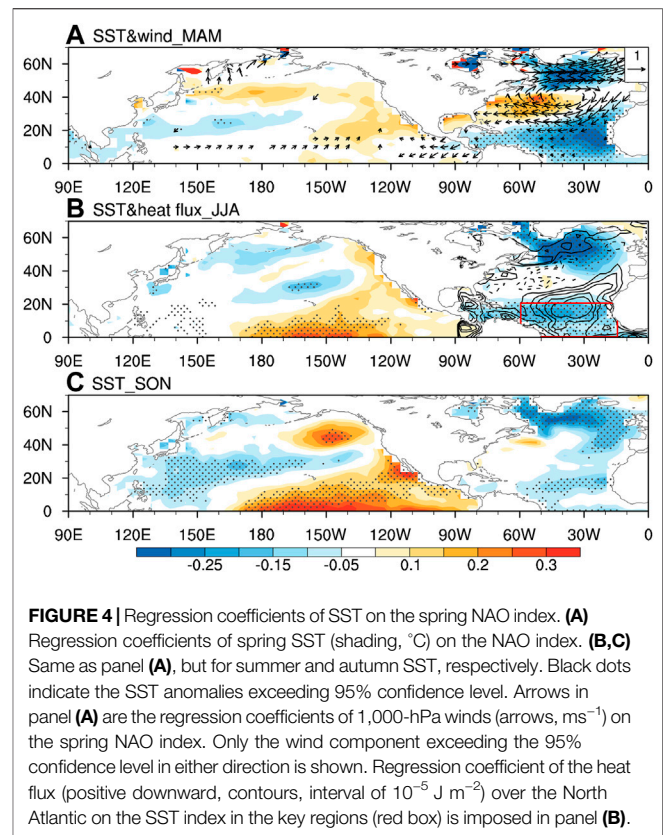
environment parameters in summer and autumn and further influence the TCGF over NA and NP. Next, we aimed to explore how the effect of the spring NAO persists into summer and autumn and plays an important role in the large-scale environment parameters closely associated with the TCGF over the NA and NP.

MECHANISM

A positive spring NAO is featured by an anti-cyclone and a cyclone over the tropical and subpolar Atlantic at 1,000 hPa, respectively (Li and Wang, 2003; **Figure 4A**). The surface easterly (westerly) wind anomalies south (north) of tropical anti-cyclone enhance the climatological easterly (westerly) wind and increase the heat flux released from the ocean to the atmosphere, leading to the local SST cooling (Zuo et al., 2013; **Figure 4A**). The negative SST anomalies can persist from spring to summer *via* the ocean memory and cool the atmosphere in summer through the heat flux (Wu et al., 2009; **Figure 4B**). This suggests that the spring NAO may impose significant influences on the environmental parameters associated with the TCGF *via* the NA SST in summer. Accordingly, the area-averaged negative SST anomalies over (60.5°W–15.5°W, 0.5°N–20.5°N), which persist from spring to summer, is defined as the SST index to further analyze how the spring NAO influence the TCGF *via* the summer NA SST. For the convenience of comparison, the sign of the SST index has been reversed. The regression coefficients of
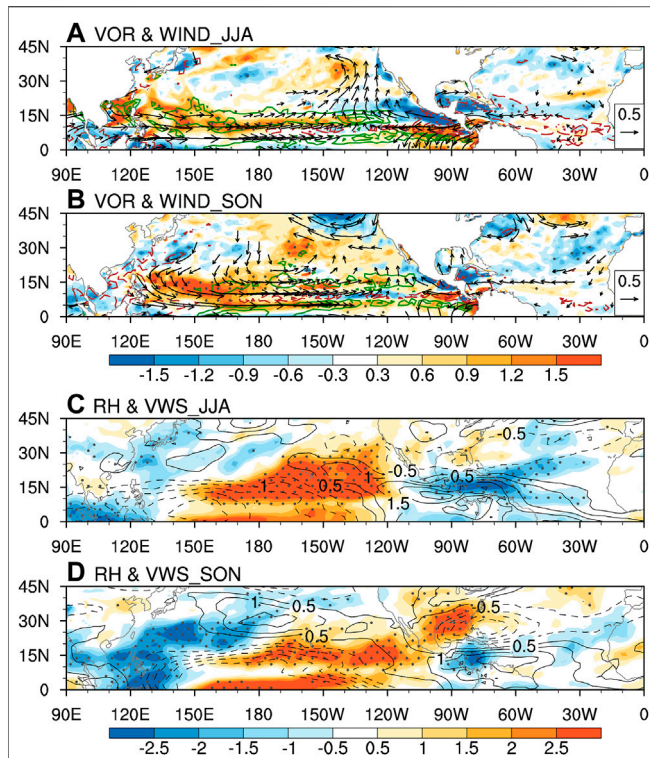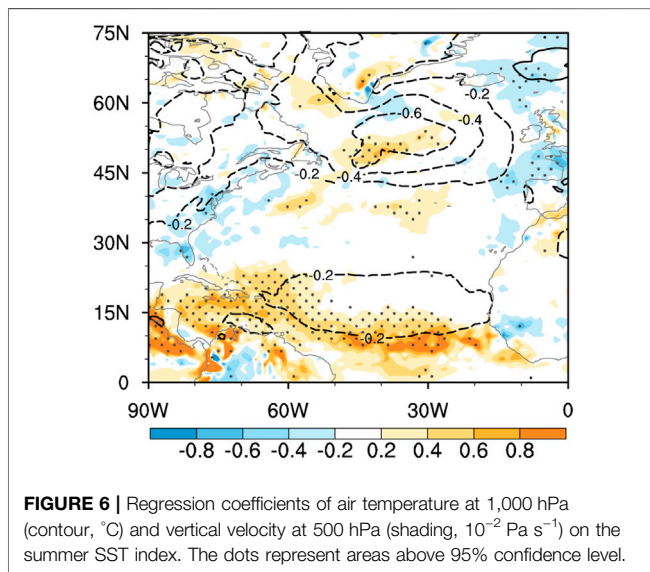
FIGURE 5 | Same as Figure 3, but for regression coefficients on the summer SST index. Brown and green contours represent the negative and positive regression coefficients of precipitation on the SST index in panels (A,B), respectively. (C,D) Same as panel (A), but for relative humidity (shading, %) and vertical wind shear (contours, interval of 0.5 m s^{-1}) in summer and in autumn, respectively. Black dots indicate the vorticity and relative humidity anomalies exceeding 95% confidence level. Only the wind component exceeding the 95% confidence level in either direction is shown in panels (A,B).
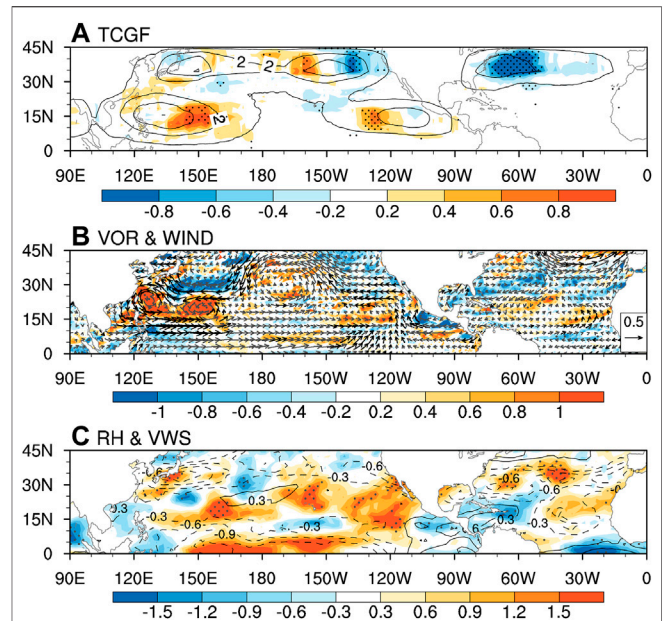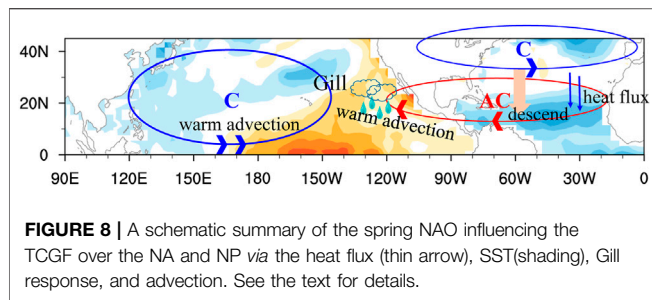

FIGURE 7 | Composite of TCGF, 850-hPa vorticity, 850-hPa winds, 600-hPa relative humidity, and vertical wind shear differences in summer and autumn between positive and negative spring NAO years in ECMWF. (A) TCGF difference between the positive and negative NAO years; (B) same as panel (A), but for 850-hPa vorticity (shading, unit: 10^{-6} s^{-1}) and 850-hPa winds (gray arrows, units: m s^{-1}) differences; (C) same as panel (B), but for 600-hPa relative humidity (shading, unit: %) and vertical wind shear (contours, units: m s^{-1}) differences. Black vectors indicate the wind component exceeding the 90% confidence level in either direction. The dots represent areas above 90% confidence level. Contours in panel (A) indicate the climatological TCGF, which starts from 0.5 with an interval of 1.5.

FIGURE 6 | Regression coefficients of air temperature at 1,000 hPa (contour, °C) and vertical velocity at 500 hPa (shading, 10^{-2} Pa s^{-1}) on the summer SST index. The dots represent areas above 95% confidence level.

vorticity, winds, relative humidity, and vertical wind shear on the summer SST index bear high similarity to those related to the spring NAO (Figures 3, 5). The negative vorticity and relative humidity with positive wind shear over the NA suppress the TCGF, while the anomalous circulations promote TCGF over the NP, forming a see-saw variability of circulations and TCGF across two basins. These confirm the bridge role of the NA SST between the spring NAO and TCGF in summer and autumn. Now, of our interest is how the SST anomaly in summer modules the large-scale conditions associated with the TCGF over the NA and NP.

Figure 6 shows the regression coefficients of air temperature at 1,000 hPa and vertical velocity at 500 hPa on the summer SST index in the NA. As expected, the negative air temperature appears over the negative SST key regions due to the heat flux anomalies (Figure 4B). The negative air temperature over the tropical NA corresponds to the anomalous descent, which benefits the anti-cyclonic circulation at lower troposphere and cyclonic circulation at upper troposphere in summer (Yu et al., 2016). These devote to the negative vorticity and relative humidity anomaly and positive vertical wind shear (Figures 5A,C), which counteract the TCGF over the NA. On the other hand, the negative air temperature and anomalous descent damp the convective activity over the tropical NA (Figure 5A), in turn forcing anti-cyclonic circulation to its northwest according to the Gill response (Gill, 1980; Ham et al., 2013). It also suppresses the TCGF over the NA and extends the NA anti-cyclonic circulation westward to the eastern Pacific (Figure 5A). Meanwhile, the

FIGURE 8 | A schematic summary of the spring NAO influencing the TCGF over the NA and NP *via* the heat flux (thin arrow), SST(shading), Gill response, and advection. See the text for details.

southerly wind anomaly west of the anti-cyclone increases the local SST (**Figure 4B**) and precipitation over the domain (150°W–120°W, 10°N–15°N; **Figure 5A**) through the warm advection from the equator. The increased diabatic heating associated with the enhanced precipitation triggers an anomalous cyclone to its northwest according to Gill response, which corresponds to the positive vorticity and relative humidity and fosters the TCGF over the NP (**Figure 5A**). The westerly wind south of the anomalous cyclone warms the tropical SST in the NP *via* transporting warm water from the warm pool (**Figure 4B**), which, in turn, enhances the cyclonic circulation *via* the Gill response. The anomalous cyclone and warmer SST in the tropical NP are enhanced *via* this air–ocean positive feedback and persist into autumn (**Figures 4C, 5B**), which benefits the NP TCGF in autumn. Yu et al. (2016) suggested that the cold NA SST anomaly can increase the TCGF in the western NP through the eastward air–sea interaction way across the Indian Ocean. We supplement that it is also feasible through the westward air–sea interaction way directly westward to the NP.

To verify the relationship between the spring NAO and TCs in summer and autumn, 35 (40) positive (negative) NAO years in five ECWMF members are selected according to the ±0.7 normalized NAO index to composite the TCGF and the associated large-scale environment parameters (**Figure 7**). The composite summer–autumn TCGF and circulation differences reproduce the observational counteracted circulation patterns over the respective NA and NP, leading to the see-saw change in TCGF across basins. The TCs significantly increases in the NP but decreases in the NA (**Figure 7A**). The positive (negative) vorticity and relative humidity with negative (positive) vertical wind shear benefit (suppress) the TCs in the NP (NA, **Figures 7B,C**). Note that the negative TCGF over the NA shifts northward and locates around 30°N compared with the observation (**Figure 1A**), which may be due to the simulation northward bias of the climatological TCGF over the NA.

Thus, the positive NAO in spring can induce negative SST anomalies over the NA, which persist into summer. In summer, the tropical negative SST anomalies lead to a low-level anti-cyclonic circulation through heat fluxes and Gill response, which damps the TCGF over the NA. Meanwhile, the anti-cyclonic circulation benefits its west precipitation; the precipitation anomalies further forced an anomalous cyclonic circulation over the NP *via* Gill response and devoted the TCGF over the NP. The westerly wind south of the anomalous cyclone warms the tropical SST in the NP and enhances the cyclone *via* the air–ocean positive feedback, which benefits the TCGF over the NP in autumn.

SUMMARY AND DISCUSSION

This study investigates the influence of spring NAO on the NH TCGF in summer and autumn and finds that positive NAO suppresses (benefits) the TCGF over the NA (NP) through modulating the vorticity, relative humidity, and vertical wind shear. The positive NAO in spring can induce negative SST anomalies over the NA, which persist into summer *via* ocean memory. The tropical negative SST anomalies cool the overlying atmosphere and damp the precipitation, leading to a low-level anti-cyclonic circulation. The anti-cyclonic circulation devotes negative vorticity, negative relative humidity, and positive vertical wind shear, all counteracting the TCGF over the NA. The southerly west of the anti-cyclonic circulation increases the local SST and precipitation. Accordingly, a cyclonic circulation appears in the western Pacific *via* Gill response. The cyclonic circulation sustains from summer to autumn *via* the warm advection by its westerly wind and fosters the TCGF in the NP (**Figure 8**).

The SST anomaly associated with the spring NAO bears some similarities to the ENSO evolution from summer to autumn (**Figure 4**; Chen et al., 2014); we further check the modulation of the ENSO on the relationship between the spring NAO and TCGF. The results are not changed with the preceding winter ENSO signal removed in advanced (not shown). Although the preceding influence of the NAO on the TCGF has been investigated by Choi and Cha (2017) and Zhou and Chen (2020), this study focuses on the NH influence rather than the western NP. More importantly, the NAO index used in this study is averaged over the spring season, which leads the summer and autumn TCGF over the NH. It implies that the NAO could be a good candidate for predicting the TC activity over the specific regions of the NH in the following typhoon season.

DATA AVAILABILITY STATEMENT

The original contributions presented in the study are included in the article/Supplementary Material, further inquiries can be directed to the corresponding author.

AUTHOR CONTRIBUTIONS

LZ and XY contributed to figures included in this manuscript. LZ and JZ wrote the manuscript. All authors contributed to the article and approved the submitted version.

FUNDING

ACKNOWLEDGMENTS

REFERENCES

Barnston, A. G., and Livezey, R. E. (1987). Classification, Seasonality and Persistence of Low-Frequency Atmospheric Circulation Patterns. *Mon. Wea. Rev.* 115, 1083–1126. doi:10.1175/1520-0493(1987)115<1083:csapol>2.0.co;2

Cao, X., Chen, S., Chen, G., and Wu, R. (2016). Intensified Impact of Northern Tropical Atlantic SST on Tropical Cyclogenesis Frequency over the Western North Pacific after the Late 1980s. *Adv. Atmos. Sci.* 33, 919–930. doi:10.1007/s00376-016-5206-z

Chan, J. C., and Xu, M. (2009). Inter-annual and Inter-decadal Variations of Landfalling Tropical Cyclones in East Asia. Part I: Time Series Analysis. *Int. J. Climatol.* 35 (11), 3353–3361. doi:10.1002/joc.1782

Chen, D., Wang, H., Liu, J., and Li, G. (2015a). Why the spring North Pacific Oscillation Is a Predictor of Typhoon Activity over the Western North Pacific. *Int. J. Climatol.* 35, 3353–3361. doi:10.1002/joc.4213

Chen, X., Wang, Y., and Zhao, K. (2015b). Synoptic Flow Patterns and Large-Scale Characteristics Associated with Rapidly Intensifying Tropical Cyclones in the South China Sea. *Mon. Weather Rev.* 143, 64–87. doi:10.1175/MWR-D-13-00338.1

Chen, G., and Huang, R. (2009). Interannual Variations in Mixed Rossby-Gravity Waves and Their Impacts on Tropical Cyclogenesis over the Western North Pacific. *J. Clim.* 22, 535–549. doi:10.1175/2008JCLI2221.1

Chen, S., Yu, B., and Chen, W. (2014). An Analysis on the Physical Process of the Influence of AO on ENSO. *Clim. Dyn.* 42, 973–989. doi:10.1007/s00382-012-1654-z

Choi, K.-S., and Byun, H.-R. (2010). Possible Relationship between Western North Pacific Tropical Cyclone Activity and Arctic Oscillation. *Theor. Appl. Climatol.* 100, 261–274. doi:10.1007/s00704-009-0187-9

Choi, J.-W., and Cha, Y. (2017). Possible Relationship between NAO and Tropical Cyclone Genesis Frequency in the Western North Pacific. *Dyn. Atmospheres Oceans* 77, 64–73. doi:10.1016/j.dynatmoce.2016.08.006

Du, Y., Yang, L., and Xie, S.-P. (2011). Tropical Indian Ocean Influence on Northwest Pacific Tropical Cyclones in Summer Following Strong El Niño*. *J. Clim.* 24, 315–322. doi:10.1175/2010JCLI3890.1

Du, Y., Zhang, J., Zhao, S., and Chen, H. (2020). Impact of the Eastward Shift in the Negative-phase NAO on Extreme Drought over Northern China in Summer. *J. Geophys. Res. Atmos.* 125, e2019JD032019. doi:10.1029/2019JD032019

Elsner, J. B., and Kocher, B. (2000). Global Tropical Cyclone Activity: a Link to the North Atlantic Oscillation. *Geophys. Res. Lett.* 27, 129–132. doi:10.1029/1999gl010893

Gill, A. E. (1980). Some Simple Solutions for Heat-Induced Tropical Circulation. *Q.J R. Met. Soc.* 106, 447–462. doi:10.1002/qj.49710644905

Gray, G. M. (1979). "Hurricanes: Their Formation, Structure and Likely Role I the Tropical Circulation," in *Meteorology over Tropical Oceans*. Editor D. B. Shaw (Bracknell: Royal Meteorological Society), 155–218.

Ham, Y.-G., Kug, J.-S., Park, J.-Y., and Jin, F.-F. (2013). Sea Surface Temperature in the north Tropical Atlantic as a Trigger for El Niño/Southern Oscillation Events. *Nat. Geosci* 6, 112–116. doi:10.1038/ngeo1686

Hersbach, H., Bell, B., Berrisford, P., Hirahara, S., Horányi, A., Muñoz-Sabater, J., et al. (2020). The ERA5 Global Reanalysis. *Q.J.R. Meteorol. Soc.* 146, 1999–2049. doi:10.1002/qj.3803

Jianping, L., and Wang, J. X. L. (2003). A New North Atlantic Oscillation index and its Variability. *Adv. Atmos. Sci.* 20, 661–676. doi:10.1007/BF02915394

Jones, P. D., Jonsson, T., and Wheeler, D. (1997). Extension to the North Atlantic Oscillation Using Early Instrumental Pressure Observations from Gibraltar and South-West Iceland. *Int. J. Climatol.* 17, 1433–1450. doi:10.1002/(sici)1097-0088(19971115)17:13<1433:aid-joc203>3.0.co;2-p

Kossin, J. P., Emanuel, K. A., and Camargo, S. J. (2016). Past and Projected Changes in Western North Pacific Tropical Cyclone Exposure. *J. Clim.* 29, 5725–5739. doi:10.1175/JCLI-D-16-0076.1

Li, T. (2012). in *Synoptic and Climatic Aspects of Tropical Cyclogenesis in Western North Pacific*. Editors K. Oouchi and H. Fudeyasu, 61–94. Chap. 3.

Lu, M., and Xiong, R. (2019). Spatiotemporal Profiling of Tropical Cyclones Genesis and Favorable Environmental Conditions in the Western Pacific Basin. *Geophys. Res. Lett.* 46, 11548–11558. doi:10.1029/2019GL084995

Maue, R. N. (2009). Northern Hemisphere Tropical Cyclone Activity. *Geophys. Res. Lett.* 36, L05805. doi:10.1029/2008GL035946

Mei, W., Kamae, Y., Xie, S.-P., and Yoshida, K. (2019). Variability and Predictability of North Atlantic Hurricane Frequency in a Large Ensemble of High-Resolution Atmospheric Simulations. *J. Clim.* 32, 3153–3167. doi:10.1175/JCLI-D-18-0554.1

Murakami, H., Vecchi, G. A., Underwood, S., Delworth, T. L., Wittenberg, A. T., Anderson, W. G., et al. (2015). Simulation and Prediction of Category 4 and 5 Hurricanes in the High-Resolution GFDL HiFLOR Coupled Climate Model*. *J. Clim.* 28, 9058–9079. doi:10.1175/JCLI-D-15-0216.1

Murakami, H., Wang, B., and Kitoh, A. (2011). Future Change of Western North Pacific Typhoons: Projections by a 20-Km-Mesh Global Atmospheric Model*. *J. Clim.* 24 (4), 1154–1169. doi:10.1175/2010JCLI3723.1

Nie, Y., Ren, H.-L., and Scaife, A. A. (2020). Enhanced Mid-to-late winter Predictability of the Storm Track Variability in the North Pacific as a Contrast with the North Atlantic. *Environ. Res. Lett.* 15, 094037. doi:10.1088/1748-9326/ab9c4d

Patricola, C. M., Chang, P., and Saravanan, R. (2016). Degree of Simulated Suppression of Atlantic Tropical Cyclones Modulated by Flavour of El Niño. *Nat. Geosci* 9, 155–160. doi:10.1038/ngeo2624

Peduzzi, P., Chatenoux, B., Dao, H., De Bono, A., Herold, C., Kossin, J., et al. (2012). Global Trends in Tropical Cyclone Risk. *Nat. Clim Change* 2, 289–294. doi:10.1038/nclimate1410

Pu, X., Chen, Q., Zhong, Q., Ding, R., and Liu, T. (2019). Influence of the North Pacific Victoria Mode on Western North Pacific Tropical Cyclone Genesis. *Clim. Dyn.* 52, 245–256. doi:10.1007/s00382-018-4129-z

Rayner, N. A. (2003). Global Analyses of Sea Surface Temperature, Sea Ice, and Night marine Air Temperature since the Late Nineteenth century. *J. Geophys. Res.* 108 (D14). doi:10.1029/2002JD002670

Schultz, L. A., and Cecil, D. J. (2009). Tropical Cyclone Tornadoes, 1950-2007. *Mon. Weather. Rev.* 137, 3471–3484. doi:10.1175/2009mwr2896.1

Tao, L., Wu, L., Wang, Y., and Yang, J. (2012). Influence of Tropical Indian Ocean Warming and ENSO on Tropical Cyclone Activity over the Western North Pacific. *J. Meteorol. Soc. Jpn.* 90, 127–144. doi:10.2151/jmsj.2012-107

Walker, G. T. (1924). Everyone's Book of the Weather. By A. Francon Williams. London (The Sheldon Press), 1923. 16°. Pp. 117. 2s. 6d. Net. *Q.J.R. Meteorol. Soc.* 50, 275. doi:10.1002/qj.49705021136

Wang, B., Xiang, B., and Lee, J.-Y. (2013). Subtropical High Predictability Establishes a Promising Way for Monsoon and Tropical Storm Predictions. *Proc. Natl. Acad. Sci.* 110, 2718–2722. doi:10.1073/pnas.1214626110

Wang, C., and Lee, S.-K. (2009). Co-variability of Tropical Cyclones in the North Atlantic and the Eastern North Pacific. *Geophys. Res. Lett.* 36, L24702. doi:10.1029/2009GL041469

Wang, C., and Wang, B. (2021). Impacts of the South Asian High on Tropical Cyclone Genesis in the South China Sea. *Clim. Dyn.* 56, 2279–2288. doi:10.1007/s00382-020-05586-8

Wang, H., Long, L., Kumar, A., Wang, W., Schemm, J.-K. E., Zhao, M., et al. (2014). How Well Do Global Climate Models Simulate the Variability of Atlantic Tropical Cyclones Associated with ENSO? *J. Clim.* 27 (15), 5673–5692. doi:10.1175/jcli-d-13-00625.1Available from: https://10.1175/JCLI-D-13-00625.1

Wang, C., Wang, L., Wang, X., Wang, D., and Wu, L. (2016). North-south Variations of Tropical Storm Genesis Locations in the Western Hemisphere. *Geophys. Res. Lett.* 43, 11367–11374. doi:10.1002/2016GL071440

Wettstein, J. J., and Wallace, J. M. (2010). Observed Patterns of Month-To-Month Storm-Track Variability and Their Relationship to the Background Flow*. *J. Atmos. Sci.* 67, 1420–1437. doi:10.1175/2009JAS3194.1

Wu, Z., Wang, B., Li, J., and Jin, F.-F. (2009). An Empirical Seasonal Prediction Model of the East Asian Summer Monsoon Using ENSO and NAO. *J. Geophys. Res.* 114, D18120. doi:10.1029/2009JD011733

Yu, J., Li, T., Tan, Z., and Zhu, Z. (2016). Effects of Tropical North Atlantic SST on Tropical Cyclone Genesis in the Western North Pacific. *Clim. Dyn.* 46, 865–877. doi:10.1007/s00382-015-2618-x

Yu, J. H., Ou, L., Chen, L., Li, L., Sun, M., Zhong, X., et al. (2021). Tropical Cyclone Genesis over the Western North Pacific Impacted by SST Anomalies from Other Basins while El Niño Decays. *Q. J. R. Meteorol. Soc.* 147, 2580–2596. doi:10.1002/qj.4042

Zhan, R., Wang, Y., and Lei, X. (2011). Contributions of ENSO and East Indian Ocean SSTA to the Interannual Variability of Northwest Pacific Tropical Cyclone Frequency*. *J. Clim.* 24, 509–521. doi:10.1175/2010jcli3808.1

Zhang, W., Villarini, G., and Vecchi, G. A. (2020). The East Asian Subtropical Jet Stream and Atlantic Tropical Cyclones. *Geophys. Res. Lett.* 47, e2020GL088851. doi:10.1029/2020GL088851

Zhao, H., and Wang, C. (2019). On the Relationship between ENSO and Tropical Cyclones in the Western North Pacific during the Boreal Summer. *Clim. Dyn.* 52, 275–288. doi:10.1007/s00382-018-4136-0

Zhao, J., Zhan, R., and Wang, Y. (2020a). Different Responses of Tropical Cyclone Tracks over the Western North Pacific and North Atlantic to Two Distinct Sea Surface Temperature Warming Patterns. *Geophys. Res. Lett.* 47 (7), e2019GL086923. doi:10.1029/2019GL086923

Zhao, J., Zhan, R., Wang, Y., Xie, S.-P., and Wu, Q. (2020b). Untangling Impacts of Global Warming and Interdecadal Pacific Oscillation on Long-Term Variability of North Pacific Tropical Cyclone Track Density. *Sci. Adv.* 6 (41), aba6813. doi:10.1126/sciadv.aba6813

Zhou, B., and Cui, X. (2014). Interdecadal Change of the Linkage between the North Atlantic Oscillation and the Tropical Cyclone Frequency over the Western North Pacific. *Sci. China Earth Sci.* 57 (9), 2148–2155. doi:10.1007/s11430-014-4862-z

Zhou, Q., and Chen, W. (2020). Unstable Relationship between spring NAO and Summer Tropical Cyclone Genesis Frequency over the Western North Pacific. *Acta Oceanol. Sin.* 39 (5), 65–76. doi:10.1007/s13131-019-1509-0

Zuo, J.-Q., Li, W.-J., Ren, H.-L., and Chen, L.-J. (2012). Change of the Relationship between the spring NAO and East Asian Summer Monsoon and its Possible Mechanism. *Chin. J. Geophys.* 55, 23–34. doi:10.1002/cjg2.1697

Zuo, J., Li, W., Sun, C., Xu, L., and Ren, H.-L. (2013). Impact of the North Atlantic Sea Surface Temperature Tripole on the East Asian Summer Monsoon. *Adv. Atmos. Sci.* 30, 1173–1186. doi:10.1007/s00376-012-2125-5